RSC Advances

PAPER

View Article Online
View Journal | View Issue

Cite this: *RSC Adv.*, 2021, **11**, 114

Adsorption of nitrification inhibitor nitrapyrin by humic acid and fulvic acid in black soil: characteristics and mechanism

Zhongqing Zhang,[a] Qiang Gao,*[a] Zhonglei Xie,*[b] Jingmin Yang[a] and Jinhua Liu[a]

The compound nitrapyrin is easily adsorbed by soil organic matter in high-organic matter soils, and this results in its effectiveness reducing significantly. In this study, the adsorption characteristics and mechanisms of nitrapyrin as an adsorptive on humic acid (HA) and fulvic acid (FA) as adsorbents were investigated. The results showed that the kinetics of adsorption of nitrapyrin on both HA and FA followed pseudo-second-order kinetic models ($R^2 \geq 0.925$, $P < 0.05$) and the adsorption process included an initial fast-adsorption stage and a slow-adsorption stage thereafter. The adsorption efficiencies of nitrapyrin on HA + FA were higher than that on HA or FA alone, and that of HA was higher than that of FA. The adsorption isotherms of nitrapyrin on HA and FA could be optimally fitted with the Langmuir equation ($R^2 \geq 0.982$, $P < 0.05$). The maximum adsorption capacities of nitrapyrin on HA, FA and HA + FA were 4896.49, 3173.70 and 4925.56 mg kg^{-1}, respectively. Synergistic adsorption of nitrapyrin in co-existing systems of HA and FA was also observed. The adsorption mechanism of nitrapyrin on both HA and FA involved hydrogen bonding and hydrophobic interaction. Therefore, HA and FA in the soil environment can adsorb a large amount of nitrapyrin and reduce its effectiveness, and they have a positive synergistic effect.

Received 13th October 2020
Accepted 21st November 2020

DOI: 10.1039/d0ra08714a

rsc.li/rsc-advances

1 Introduction

Nitrapyrin was an early-developed nitrification inhibitor with a remarkable nitrification inhibition effect.[1] To date, it has been widely studied and applied in agricultural production.[2–6] The effectiveness of nitrification inhibitors can be affected by soil clay composition, soil organic matter, pH, temperature, soil moisture content and soil microorganisms.[7–10] Soil organic matter is one of the important factors affecting the effectiveness through the adsorption of nitrification inhibitors.[11–15] Previous studies have shown that nitrapyrin was absorbed by organic matter in agricultural soils,[16] especially in high-organic matter soils, and its effectiveness was significantly reduced.[17–19] Nowadays, the research in this field is still focused on the following aspects: (1) the comparative analysis of the application effect of nitrapyrin in different soil types and (2) the adsorption characteristics of nitrapyrin on soil with different organic matter contents. For example, Yan *et al.*[20] compared and analyzed the nitrification inhibition effect of nitrapyrin on sandy and clay soils with different organic matter contents, and the overall performance was found to be better on sandy soil than on clay soil; Zhang *et al.*[21] found that the maximum adsorption capacity and adsorption constant of nitrapyrin on black soil before and after organic matter removal showed a significant quadratic function correlation. Zhang *et al.*[22] found that the adsorption kinetics of nitrapyrin on black soil, chernozem and planosol could be fitted using the quasi-second-order kinetic equation with a lower active energy of adsorption. The isotherm was fitted using the Langmuir equation. Temperature affected the adsorption of nitrapyrin on these three soils, and the maximum adsorption observed at different temperatures followed the order of black soil > planosol > chernozem.

The availability and environmental fate of chemical substances applied to soils are controlled by their adsorption process, which depends on the physical and chemical properties of the soil, including the content and composition of the soil organic matter, particularly the natural macromolecular organic compounds in soils.[23] Soil organic matter contains a large number of carboxyl, hydroxyl, carbonyl and other active functional groups, which play an important role in the accumulation, migration, transformation and bioavailability of organic substances in the environment.[24,25] Similarly, the effectiveness of nitrification inhibitors entering the soil environment is also affected by soil composition.[26] For example, Jacinthe *et al.*[27] studied the adsorption mechanisms of nitrapyrin on humic acid (HA), pointing out that adsorption mainly occurs through an ionic bonding mechanism. At present, the

[a]*Key Laboratory of Soil Resource Sustainable Utilization for Jilin Province Commodity Grain Bases, College of Resources and Environmental Science, Jilin Agricultural University, Xincheng Road 2888, Changchun 130118, China. E-mail: jlauzy2019@163.com*

[b]*College of Plant Science, Jilin University, Changchun, 130062, China. E-mail: xiezl@jlu.edu.cn*

synergistic effect of HA and fulvic acid (FA) in nitrapyrin adsorption and the underlying mechanism are still unclear. Northeast China hosts China's Golden Corn Belt, which is one of the three major black soil regions in the world. The soil organic matter content is high. The fertilization method "one fertilizer application" used by the local farmers results in a lower utilization rate of nitrogen fertilizer.[28,29] Under the nitrogen fertilizer reduction policy formulated by the Chinese government, chemical fertilizers contain a certain amount of N. Nitrification inhibitors such as nitrapyrin are an effective tool to improve the utilization rate of nitrogen fertilizers and reduce the use of nitrogen fertilizers. Therefore, it is necessary to study the adsorption of nitrapyrin on soil organic matter with different components and its mechanism at the molecular level. In this study, the classical batch equilibrium method and modern analytical techniques were combined to explore the characteristics and mechanism of nitrapyrin adsorption on HA and FA. This will provide a theoretical basis for elucidating the adsorption mechanism of nitrapyrin in a high soil organic matter environment.

2 Materials and methods

2.1 HA and FA preparation from black soil

The extraction, separation and purification of HA and FA from black soil were carried out according to Wen *et al.*[30] and Xing *et al.*[31] The black soil was obtained from Hailun City, Heilongjiang Province (E126°50′55″, N47°26′31″). Corn has been planted there for many years without application of the nitrification inhibitor nitrapyrin. The soil was sampled at a depth of 0–20 cm, and the undecomposed plant residues on the soil surface were removed manually. The underlying physical and chemical properties of the soil are summarized in Table 1.

2.2 Chemicals and instruments

Ethanol, analytically pure, purchased from the Beijing Chemical Co., Ltd.; acetonitrile, chromatographically pure, obtained from Shandong Yuwang and World New Materials Co., Ltd; nitrapyrin raw medicine (98.0%), purchased from the Wuhan Yuancheng Gongchuang Technology Co., Ltd.; the standard of nitrapyrin (99.0%), purchased from LGC Labort GmbH Bgm, Germany; calcium chloride, analytically pure, obtained from the Huoguo Pharmaceutical Group Co., Ltd. The water used in the experiments was double-distilled water. High-performance liquid chromatography (HPLC, Agilent 1260, SB-C18 stainless steel columns, USA); high-speed refrigeration centrifuge (Z36HK, HERMLE); constant-temperature water bath oscillator (SHA-C, Huapuda Instrument Co., Ltd.); infrared spectroscopy (FTIR-IR, Affinity-1S, Japan); scanning electron microscopy (JSM-7900F, Japan); X-ray energy dispersive spectrometry (C-Max, EDS).

2.3 Adsorption kinetics

1.0000 g of HA, FA or HA + FA (1 : 1) was added into a 50 mL plugged centrifuge tube. 50 mg L^{-1} nitrapyrin was added to the soil (the solution comprised 0.01 mol L^{-1} $CaCl_2$ and an ethanol/water mixture (v/v = 5 : 95)), and this was repeated three times in combination with oscillation under dark conditions (constant-temperature water bath oscillator, 200 rpm) at 298 K. The acting time was 5, 10, 30, 60, 120, 240, 360, 480, 720, and 1440 min. The samples were centrifuged at a speed of 10 000 rpm after 5 min. The supernatant was filtered out by a 0.45 μm organic filter membrane and sealed in a brown spectrographic bottle stored in the dark at 3 °C, to determine the content of nitrapyrin by HPLC. For further details on the methods, refer to our previously published research results.[21,22]

2.4 Adsorption thermodynamics

1.0000 g samples of HA, FA and HA + FA (1 : 1) were accurately weighed and placed in a 50 mL plugged centrifuge tube. 25 mL of nitrapyrin solution (0.01 mol L^{-1} $CaCl_2$ and an ethanol/water solution (v/v = 5 : 95)) was added. The concentration of the nitrapyrin solution was 0, 5, 10, 15, 25, 50 and 75 mg L^{-1}. The treatments were repeated three times, and the samples were placed in a constant-temperature water bath oscillator. The adsorption experiments were carried out at different reaction temperatures (298, 308, and 318 K) at a 200 rpm oscillation speed. After 24 hours, the samples were centrifuged at a speed of 10 000 rpm. The supernatant was filtered by a 0.45 μm organic filter membrane and sealed in a brown bottle. The supernatant was stored in the dark at 3 °C, and the content of nitrapyrin was determined by HPLC. The remaining solid samples in the centrifuge tube were dried at 50 °C for surface morphology analysis, and element distribution and functional group composition determination. For details of the research methods, refer to our previous published research results.[21,22]

2.5 HPLC conditions

The HPLC conditions were as follows:[32–34] the detector, UV-Vis (Agilent 1260, US); the wavelength, 285 μm; the chromatographic column, ^{18}C column (4.6 × 150 mm, 5 μm, Agilent Pursuit); the column temperature, 25 °C; the mobile phase, acetonitrile/water (8/2); the flow rate, 0.8 mL min^{-1}; the injection volume, 20 μL. The concentration gradient of nitrapyrin was 2, 4, 8, 10, 15, 25, 50 and 75 mg L^{-1}.

Table 1 Basic physicochemical properties of the black soil

Soil type	pH	Organic matter (g kg^{-1})	*N* (g kg^{-1})	P_2O_5 (g kg^{-1})	K_2O (g kg^{-1})
Black soil	6.55	48.51	13.51	3.23	1.54

2.6 Characterization of HA and FA

The surface morphology of HA/HA–nitrapyrin and FA/FA–nitrapyrin complexes was observed using scanning electron microscopy (JSM-7900F, Japan). The element distribution was determined by using X-ray energy dispersive spectroscopy (C-Max, EDS). The infrared spectra of HA/HA–nitrapyrin and FA/FA–nitrapyrin complexes were recorded using Fourier transform infrared spectroscopy (ftir-IRAffinity-1S, Japan).

2.7 Data processing method

Origin 8.5 software was used to fit the data. An Agilent workstation (Chem Station Edition for LC and LC/MS systems, C0.01.05 (ref. 35)) was used to obtain the chromatogram of nitrapyrin.

(1) Adsorption kinetics model

Quasi-first-order dynamics:

$$\ln(q_e - q_t) = \ln q_{e1} - k_1 t \quad (1)$$

Quasi-second-order dynamics:

$$t/q_t = 1/k_2 q_e^2 + t/q_e \quad (2)$$

Elovich equation:

$$q_t = a + b_t \quad (3)$$

"q_t" is the adsorption amount when time is t (mg kg^{-1}). "t" is the adsorption time (min). "a, k" is a model parameter. "q_e" is the maximum adsorption capacity (mg kg^{-1}). "A" is a constant related to the initial rate of reaction. "b" is a constant related to the activation energy of adsorption.

(2) Adsorption isothermal equation/adsorption thermodynamic equation

Langmuir:

$$Q_d = k_1 Q_{d0} C_d/(1 + k_1 C_d) \quad (4)$$

Freundlich:

$$Q_d = k_f C_d^{1/n} \quad (5)$$

Q_d represents the adsorption amount (mg kg^{-1}), C_d is the adsorption equilibrium solution concentration (mg L^{-1}), Q_{d0} is the maximum adsorption capacity (mg kg^{-1}), and k is a constant.

(3) Gibbs free energy change of adsorption

$$\Delta G^\circ = -RT \ln k_1 \quad (6)$$

$$\Delta H^\circ = R[T_2 T_1/(T_2 - T_1)], \ln(k_{1(T_2)}/k_{1(T_1)}) \quad (7)$$

$$\Delta S^\circ = (\Delta H^\circ - \Delta G^\circ)/T \quad (8)$$

ΔG° is the free energy change (kJ mol^{-1}), ΔH° is the enthalpy change (kJ mol^{-1}), ΔS° is the entropy change (J mol^{-1} K^{-1}), R is the universal gas constant (8.314 J K^{-1} mol^{-1}), T is the absolute temperature (K), and k_1 is the equilibrium constant (L mol^{-1}) of the Langmuir equation.

3 Results and discussion

3.1 Adsorption kinetics of nitrapyrin on HA and FA

The adsorption of pyridine organic compounds (AM, chloropyralid, *etc.*) on soil organic matter conforms to an initial rapid adsorption and a later slow adsorption.[35–37] The adsorption kinetics of nitrapyrin on HA, FA and HA + FA of black soil at 298 K showed that the adsorption process comprised an initial fast adsorption stage and a subsequent slow adsorption stage (Fig. 1). The adsorption equilibrium state was basically reached at 750 min. The adsorption capacity of HA + FA for nitrapyrin was greater than that of HA or FA, and that of HA was greater than that of FA. The nitrapyrin was mainly adsorbed on the outer surface of HA and FA in the fast adsorption stage. This process occurs due to the radial movement of nitrapyrin molecules with the minimum diffusion resistance, and the adsorption rate is fast. In the slow adsorption stage, due to the great resistance of HA with a narrow pore size, the diffusion speed of nitrapyrin through HA and FA was slow, the adsorption rate was slow, and the adsorption equilibrium state was reached gradually.

The adsorption kinetics of nitrapyrin on HA, FA and HA + FA can be fitted by the quasi-first-order kinetic equation, quasi-second-order kinetic equation and Elovich equation, respectively. Previous studies found that the adsorption kinetics of organic compounds on soil or soil organic matter conforms to the quasi-second-order kinetic equation.[26,37–40] The adsorption kinetics of nitrapyrin on HA, FA and HA + FA fit the quasi-second-order kinetic equation best ($P < 0.05$), and the fit equilibrium adsorption capacity was consistent with the experimental results (Table 2). The quasi-second-order kinetic equation fitting effect of nitrapyrin on HA + FA was better than on HA or FA, and that of HA was better than that of FA.

3.2 Thermodynamics of nitrapyrin on HA and FA

The adsorption isotherms of HA, FA and HA + FA at different temperatures (298 K, 308 K and 318 K) are shown in Fig. 2. With the increase of nitrapyrin concentration and temperature, the

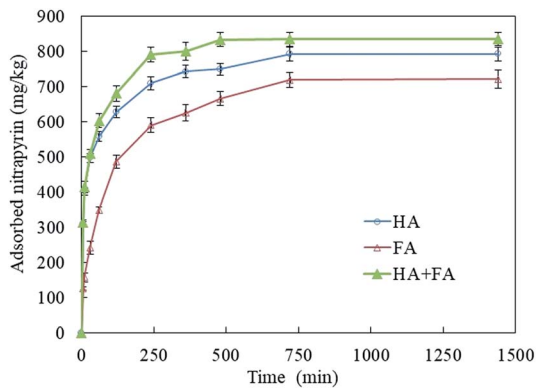

Fig. 1 Absorption kinetics of nitrapyrin on HA, FA and HA + FA (298 K).

Table 2 Adsorption kinetics model parameters of nitrapyrin on HA, FA and HA + FA

	Quasi-first-order dynamic equation			Quasi-second-order dynamic equation			Elovich equation		
Treatment	q_e (mg kg^{-1})	k_1	R^2	q_e (mg kg^{-1})	k_2	R^2	a	b	R^2
HA	616.84	115.9	0.52	747.76	0.00013	0.955	187.44	90.23	0.881
FA	467.39	88.4	0.212	747.70	0.00002	0.925	−113.06	121.98	0.879
HA + FA	638.56	122.4	0.420	752.26	0.00014	0.973	111.12	73.33	0.885

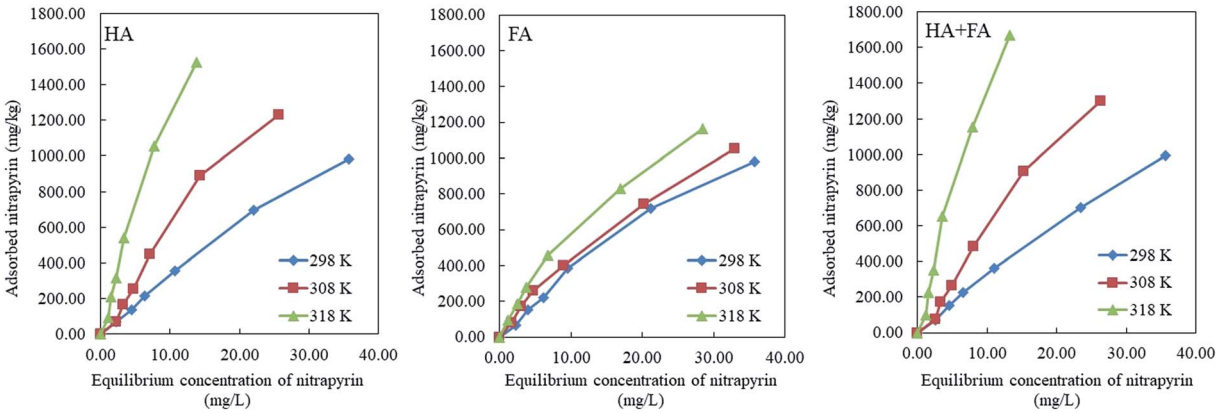

Fig. 2 Adsorption isotherms of nitrapyrin on HA, FA and HA + FA.

adsorption capacity of HA, FA, and HA + FA for nitrapyrin increased at different rates.

The adsorption isotherms of nitrapyrin on HA, FA and HA + FA were fitted using the Langmuir and Freundlich equations, respectively. Table 3 shows that both the Langmuir and Freundlich equations can be used to fit the adsorption isotherms of nitrapyrin on HA, FA and HA + FA ($R^2 > 0.9300$, $P < 0.05$). The maximum adsorption capacities of nitrapyrin on HA, FA and HA + FA were 4896.49, 3173.70 and 4925.56 mg kg^{-1}, respectively. The adsorption capacity of nitrapyrin on HA was higher than that on FA, which was consistent with the previous research.[27] However, the adsorption capacity of nitrapyrin on HA + FA was greater than that on HA or FA alone, indicating that there was a positive synergistic effect on the adsorption of nitrapyrin due to the co-existence of HA and FA. The constant $n > 1$ obtained using the Freundlich equation confirmed that both HA and FA can adsorb nitrapyrin easily, and leads to an L-type isotherm curve. This indicated that nitrapyrin molecules occupy the adsorption sites of HA, FA and HA + FA quickly at the beginning of adsorption, and that surface adsorption was the main type of adsorption. With an increase of reaction temperature, the Langmuir isotherm parameters showed an increasing trend, which indicated that the increase of temperature could promote the adsorption of nitrapyrin by HA, FA and HA + FA. For the adsorption of organic compounds on HA or FA, generally, the Langmuir isotherm parameters increase with an increase of reaction temperature.[39–41] The increase of temperature promoted the diffusion of nitrapyrin molecules, reduced the solution viscosity, and promoted the entry of nitrapyrin molecules into

Table 3 Adsorption isotherm equation parameters of nitrapyrin on HA, FA and HA + FA

		Langmuir model			Freundlich model		
Treatment	Temperature (K)	q_m (mg kg^{-1})	k_L (L mg^{-1})	R^2	k_F [mg kg^{-1} (L mg^{-1})$^{-1/n}$]	n	R^2
HA	298	4152.17	2024.61	0.998	2249.09	1.14	0.995
	308	4708.66	3300.47	0.982	3883.62	1.14	0.974
	318	4896.49	7718.63	0.991	5746.09	1.19	0.984
FA	298	2665.34	3849.25	0.995	1150.78	1.25	0.988
	308	3046.12	3923.39	0.995	1247.39	1.26	0.998
	318	3173.70	5140.42	0.997	1379.93	1.29	0.999
HA + FA	298	4189.56	2058.96	0.993	2263.26	1.19	0.992
	308	4793.65	3349.69	0.989	3895.69	1.18	0.980
	318	4925.56	7798.36	0.990	5798.62	1.21	0.979

Table 4 Thermodynamic parameters of nitrapyrin adsorption on HA, FA and HA + FA

Treatment	Temperature (K)	Adsorption thermodynamic parameters ΔG° (kJ mol^{-1})	ΔH° (kJ mol^{-1})	ΔS° (J mol^{-1} K^{-1})
HA	298	−34.77	19.52	292.10
	308	−37.19		
	318	−38.82		
FA	298	−36.31	5.01	144.70
	308	−37.62		
	318	−39.57		
HA + FA	298	−32.72	20.35	301.21
	308	−35.11		
	318	−36.85		

the internal pores through the outer boundary of the adsorbent.[42,43] In addition, the effect of temperature on the adsorption of nitrapyrin on HA was greater than that on FA.

The thermodynamic parameters of adsorption obtained by linear calculation of $\Delta G^\circ - T$ are shown in Table 4. ΔG° was negative, and the absolute value of ΔG° increased with an increase of temperature, which indicated that the process of nitrapyrin chemisorption by HA, FA and HA + FA was spontaneous with an increase of temperature. The absolute value of ΔG° was less than 40 kJ mol^{-1}, which indicated that the adsorption of nitrapyrin by HA, FA and HA + FA was mainly physical adsorption.[44] The enthalpy change of adsorption (ΔH°) results indicated that the forces responsible for the adsorption of nitrapyrin on HA, FA and HA + FA were different, but were mainly hydrogen bonding, hydrophobic interaction and dipole interaction. The positive value of ΔS° indicates that the increase of entropy change of nitrapyrin not adsorbed by HA, FA and HA + FA was greater than that of nitrapyrin adsorbed by HA and FA in the process of nitrapyrin adsorption.

3.3 Adsorption mechanism of nitrapyrin on HA and FA

(1) SEM analysis

The SEM images of HA, HA–nitrapyrin, FA and FA–nitrapyrin are shown in Fig. 3. HA has a fluffy, rough and porous surface structure (a). After adsorption of nitrapyrin, the surface structure of HA changed, a granular agglomerated structure formed, and some sediment appeared on the surface (b). It is possible that nitrapyrin may undergo chemisorption on the HA surface and the appearance of surface agglomeration was probably due to the reaction between the chemical groups on the HA surface and nitrapyrin, and the formation of new substances attached to the surface of HA. Fig. 3(c) and (d) show the SEM scanning results before and after nitrapyrin adsorption on FA. Before adsorption, FA had an irregular granular structure with a fluffy, rough and porous surface (c); after adsorption of nitrapyrin, the FA surface structure exhibited agglomeration, the particles became tightly bound, and the rough porous surface structure became smooth and compact (d). This indicated that nitrapyrin underwent physical adsorption on the FA surface and the appearance of surface agglomeration should be related to a decrease of the number of negative charges on the surface of FA after adsorption of nitrapyrin, thus reducing the repulsive force between molecules.

(2) EDS analysis

According to the elemental results, the unabsorbed HA contains more carbon and oxygen related functional groups, with the contents of 19.56% and 35.26%, respectively (Table 5). After adsorption, the mass and atomic percentage of carbon and oxygen decreased obviously (Table 5), which resulted from the adsorption reaction of the functional groups containing carbon and oxygen with nitrapyrin. The mass and atomic percentage of sodium and aluminum increased, indicating that the two metal elements were closely combined with the organic components of HA and were difficult to exchange into the solution. The mass and atomic percentage of chlorine increased significantly (Table 5), which also confirmed that

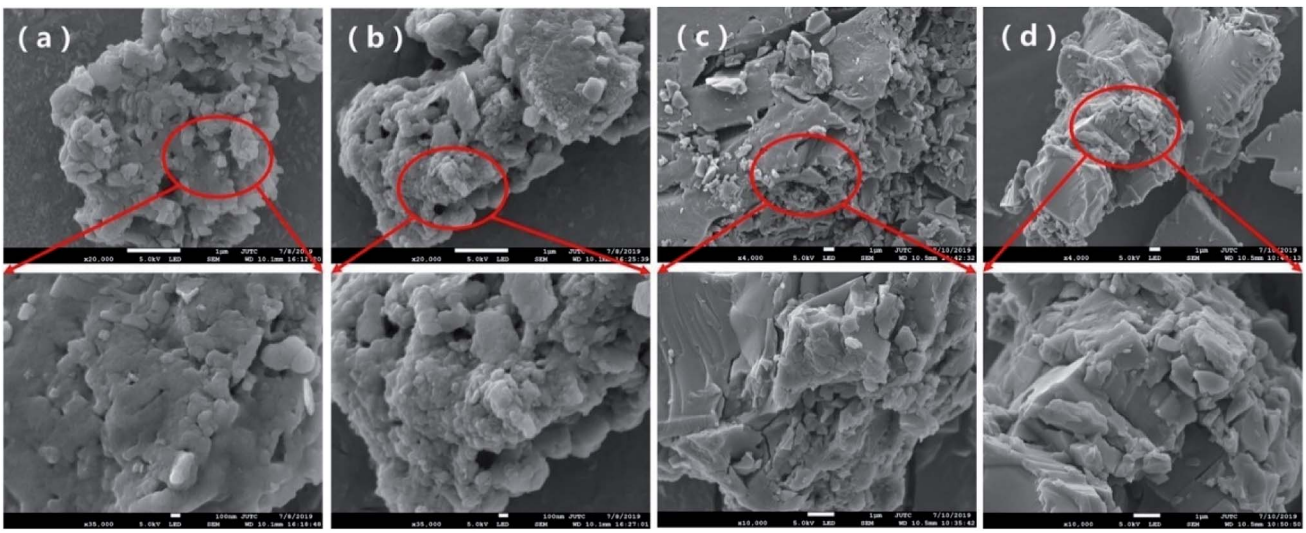

Fig. 3 SEM images of (a) HA, (b) HA–nitrapyrin, (c) FA and (d) FA–nitrapyrin.

Table 5 Elemental distribution of HA, HA–nitrapyrin, FA and FA–nitrapyrin

		Before adsorption			After adsorption		
Treatment	Element	wt (%)	wt sigma (%)	Atomic percentage (%)	wt (%)	wt sigma (%)	Atomic percentage (%)
HA	C	19.56	1.46	30.57	14.84	2.90	24.35
	O	35.26	0.67	41.40	21.05	0.91	32.11
	Na	1.15	0.06	0.94	4.03	0.13	3.71
	Al	5.90	0.12	4.11	6.55	0.17	4.80
	Si	34.72	0.66	23.25	25.74	0.60	18.75
	S	0.23	0.04	0.13	2.91	0.11	1.93
	Cl	0.77	0.05	0.41	1.85	0.07	1.13
FA	C	52.14	1.16	66.02	49.90	1.64	66.00
	O	28.24	0.73	26.85	26.14	0.87	25.90
	Si	0.09	0.02	0.04	0.20	0.03	0.12
	S	4.99	0.16	3.10	6.20	0.22	3.08
	Cl	0.86	0.05	0.47	2.00	0.08	0.90

nitrapyrin was adsorbed on HA because nitrapyrin contains a lot of chlorine.

The contents of carbon and oxygen in the unabsorbed FA were 52.14% and 28.24%, respectively (Table 5), indicating that FA contained more carbon and oxygen related functional groups. After adsorption, the mass and atomic percentage of carbon and oxygen in FA decreased (Table 5), indicating that the functional groups containing carbon and oxygen participated in the adsorption reaction with nitrapyrin. The mass and atomic percentage of chlorine in FA increased evidently (Table 5), which indicated that nitrapyrin was greatly absorbed because of the large amount of chlorine in nitrapyrin attached to FA.

(3) FTIR analysis

Fig. 4(a) shows the infrared spectra of HA and the HA–nitrapyrin complex, with the band at 3400 cm^{-1} representing the –OH bond and N–H stretching vibration, the band at 2920 cm^{-1} representing asymmetric aliphatic C–H stretching vibration, the band at 2850 cm^{-1} belonging to $-CH_2-$ symmetric stretching vibration, the band at 1720 cm^{-1} representing carboxyl C=O stretching vibration, the band at 1620 cm^{-1} representing carboxyl C=O stretching vibration, the band at 1257 cm^{-1} representing C–O stretching vibration and O–H deformation vibration related to the carboxylic acid functional group, and the bands at 914 cm^{-1} and 757 cm^{-1} representing external bending vibrations of carboxylic acid O–H and aromatic hydrocarbon C–H groups, respectively. Further, the band at 617 cm^{-1} represents an external bending vibration formed by alcohol hydroxyl groups.[45,46] Two new absorption bands at 2360 cm^{-1} and 625 cm^{-1} were found in the spectra of HA–nitrapyrin, which were attributed to the bonding of quaternary ammonium salts and the extension of C–C bonding, respectively. The increase of absorption intensity observed near 2100 cm^{-1} is a direct effect of nitrapyrin, which produces a strong absorption band in this region. Fig. 4(b) shows the spectra of FA and the FA–nitrapyrin complex, with aliphatic $-CH_2-$ asymmetric and symmetrical resonance absorption peaks at 2920 cm^{-1} and 2860 cm^{-1}, C=C vibration absorption of the aromatic ring skeleton at 1650 cm^{-1} and stretching

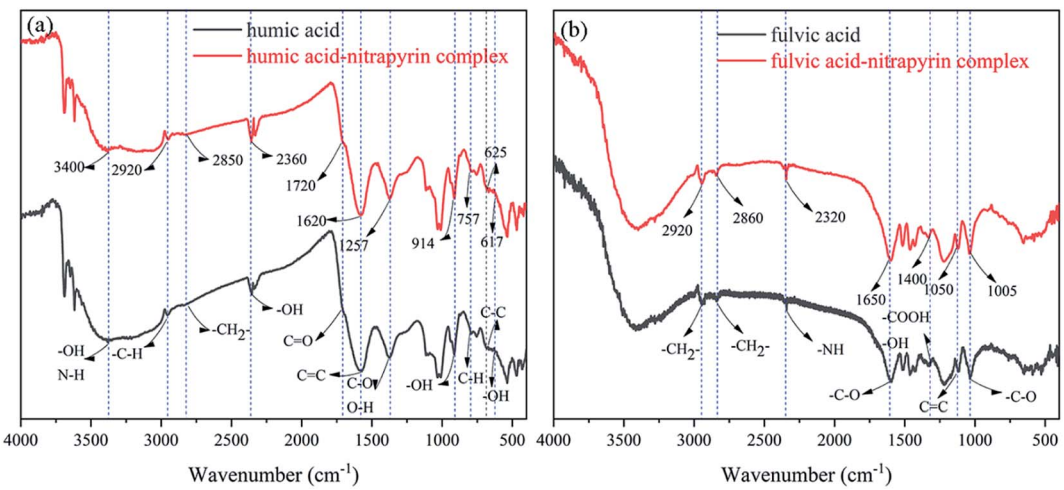

Fig. 4 FTIR spectra of (a) HA and HA–nitrapyrin, and (b) FA and FA–nitrapyrin.

vibration of –C–O- polysaccharide at 1000 cm^{-1}. The special features of the FA–nitrapyrin spectrum included the disappearance of the shoulder at 1725 cm^{-1} and a remodeling of the band near 1400 cm^{-1}, indicating that the –COOH and –OH groups of FA participate in the adsorption of nitrapyrin. The absorption intensity increased at 1650 cm^{-1}, which should be due to the interaction between the C–O group of FA and the pyridine ring of nitrapyrin. The FA–nitrapyrin complex had multiple absorption bands at 2320 cm^{-1}, which was attributed to the NH stretching effect of the pyridinium salt.

(4) Adsorption mechanism

HA and FA are the main components of soil organic matter, and they contain various organic functional groups such as carboxyl and hydroxyl groups and so on (Liu *et al.*, 2017).[39] The

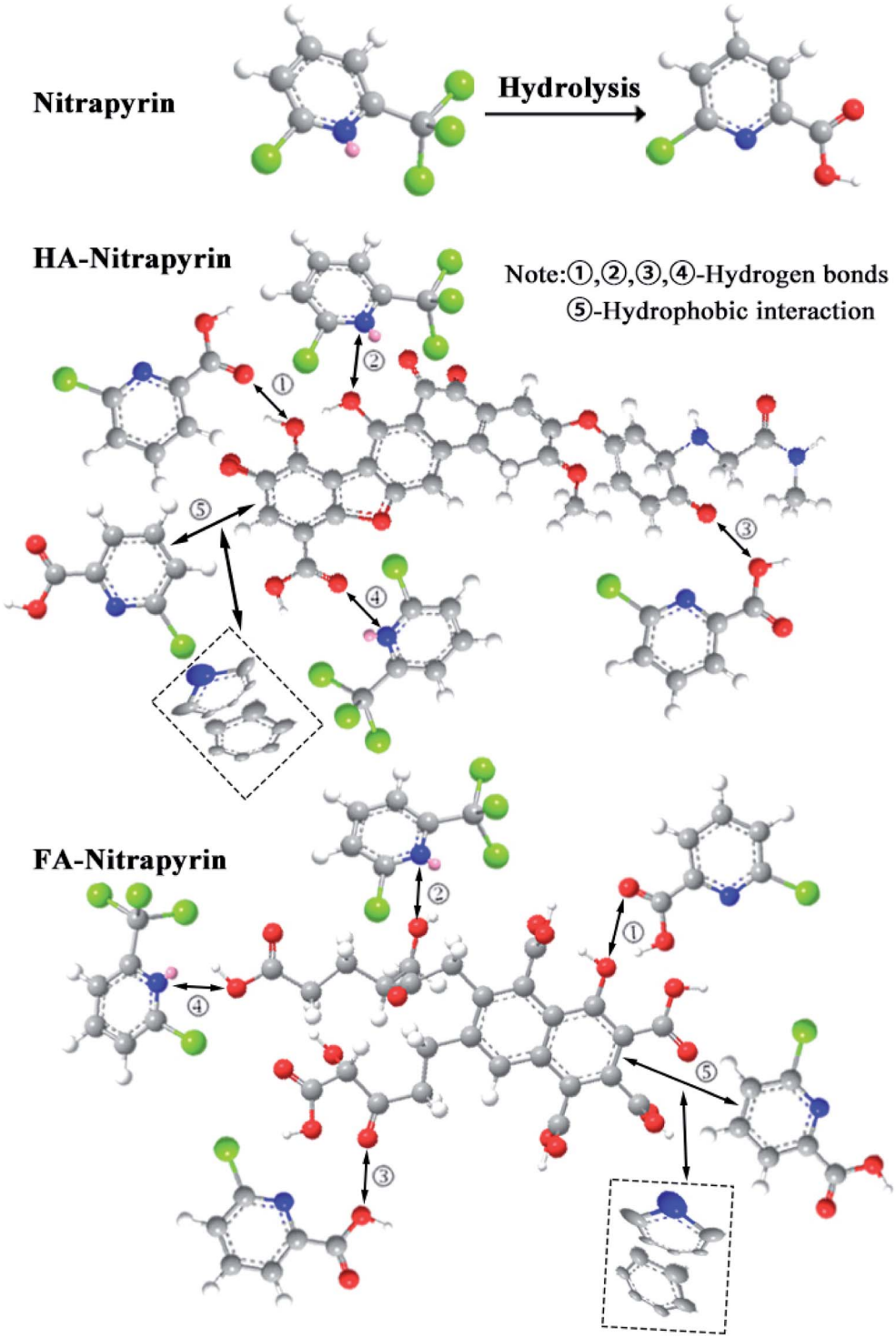

Fig. 5 Plausible interaction mechanism between HA, FA and nitrapyrin.

presence of these functional groups can lead to complex interactions of HA and FA with nitrapyrin. The adsorption isotherm study showed that the maximum adsorption capacity of nitrapyrin on HA was greater than that on FA, which was probably due to the fact that the number of oxygen-containing functional groups in HA was greater than that in FA (Table 2). The adsorption capacity for nitrapyrin in HA + FA was greater than that of HA or FA alone, which should be related to a positive synergistic effect on the adsorption of nitrapyrin due to the co-existence of HA and FA. Fig. 3 shows that the surface structure of HA and FA changed significantly before and after adsorption, indicating that there was strong interaction between some functional groups of HA and FA and nitrapyrin. The infrared spectra (Fig. 4) show that O–H (3390 cm^{-1}) and C–O (1118 cm^{-1}) are the main components of HA–nitrapyrin and FA–nitrapyrin. This indicated that the mechanism of adsorption included hydrogen bond interaction between aromatic carboxyl groups or hydroxyl groups on HA and FA, nitrogen with lone pair electrons on nitrapyrin and oxygen in hydrolyzed carboxyl groups (Fig. 5). The pyridine ring of nitrapyrin contacts with the benzene ring face-to-face, which results in effective adsorption of nitrapyrin on HA and FA through hydrophobic interaction (Fig. 5). Therefore, hydrogen bonding and hydrophobic interaction should be the most important adsorption pathways of nitrapyrin on HA and FA, and the change of adsorption enthalpy also showed that hydrogen bonding and hydrophobic interaction were the main adsorption forces. Meanwhile, the absolute values of free energy of nitrapyrin adsorbed on HA, FA and HA + FA ranged from 34.77 to 39.57 kJ mol^{-1}, indicating that the dipole moment, electrostatic interaction and ion exchange interaction were secondary factors affecting the adsorption of nitrapyrin on HA, FA and HA + FA.

4 Conclusion

The kinetics of adsorption of nitrapyrin on both HA and FA followed pseudo-second-order kinetic models ($R^2 \geq 0.925$, $P < 0.05$) and the adsorption process included an initial fast-adsorption stage and a slow-adsorption stage thereafter. The adsorption efficiencies of HA + FA for nitrapyrin were higher than that of HA or FA alone, and that of HA was higher than that of FA. The adsorption isotherms of nitrapyrin on HA and FA could be optimally fitted with the Langmuir equation ($R^2 \geq 0.982$, $P < 0.05$). The maximum adsorption capacities of nitrapyrin on HA + FA were the largest. The adsorption of nitrapyrin on co-existing systems of HA and FA involves a positive synergistic effect. The adsorption of nitrapyrin on HA and FA occurred through hydrogen bonding and hydrophobic interaction.

Conflicts of interest

There are no conflicts to declare.

Acknowledgements

The present study was supported by grants from the National Key Research and Development Program of China (2016YFD0200403) and the Scientific Technology Development Research Plan Project of Jilin Province in China (20180201035NY).

References

1 C. A. I. Goring, Control of nitrification by 2-chloro-6-(trichloro-methyl)pyridine, *Soil Sci.*, 1962, **93**(3), 211–218.
2 L. M. Fisk, L. D. Maccarone, L. Barton and D. V. Murphy, Nitrapyrin decreased nitrification of nitrogen released from soil organic matter but not amoa gene abundance at high soil temperature, *Soil Biol. Biochem.*, 2015, **88**, 214–223.
3 R. Degenhardt, L. T. Juras and L. R. Smith, Application of Nitrapyrin with Banded Urea, Urea Ammonium Nitrate, and Ammonia Delays Nitrification and Reduces Nitrogen Loss in Canadian Soils, *Crop, Forage Turfgrass Manage.*, 2016, **8**(11), 1–11.
4 S. S. Wei, Y. Q. Wang, Y. C. Li, X. X. Shu, Z. P. Peng, X. L. Shi and M. X. Men, Nitrapyrin-urea application amount with less soil N_2O emission and highest profit in summer maize and winter wheat, *Journal of Plant Nutrition and Fertilizer*, 2017, **23**(1), 231–237.
5 B. Z. Ren, J. W. Zhang, S. T. Dong, P. Liu, B. Zhao and H. Li, Nitrapyrin improves grain yield and nitrogen use efficiency of summer maize waterlogged in the field, *Agron. J.*, 2017, **109**(1), 185–192.
6 M. R. Martins, S. A. C. Sant'Anna, M. Zaman, R. C. Santos, R. C. Monteiro, B. J. R. Alves, C. P. Jantalia, R. M. Boddey and S. Urquiaga, Strategies for the use of urease and nitrification inhibitors with urea: Impact on N_2O and NH_3 emissions, fertilizer-^{15}N recovery and maize yield in a tropical soil, *Agric., Ecosyst. Environ.*, 2017, **247**, 54–62.
7 Z. M. Sun, Z. J. Wu, L. J. Chen and L. B. Jia, Regulation of soil nitrification with nitrification inhibitors and related mechanisms, *Chin. J. Appl. Ecol.*, 2008, **19**(6), 1611–1618.
8 Z. J. Wu, Y. F. Shi and L. J. Chen, Research progress of the mechanisms of nitrification inhibition, *Chin. J. Soil Sci.*, 2008, **39**(4), 962–970.
9 Z. S. Shen, X. Chao, H. T. Tang, F. Q. Huang, Y. L. Liao, Y. T. Sun and F. F. Gao, Environmental effects, influencing factors and mechanism of DMPP application, *Hunan Agricultural Sciences*, 2011, (8), 71–76.
10 Y. Gu, L. H. Wu and Z. P. Hu, Inhibitory effect of soil pH value and moisture on soil nitrification by nitrapyrin application, *J. Agric. Eng. Res.*, 2018, (8), 132–138.
11 K. Puttanna, N. M. N. Gowda and E. V. S. P. Rao, Effect of concentration, temperature, moisture, liming and organic matter on the efficacy of the nitrification inhibitors benzotriazole, *o*-nitrophenol, *m*-nitroaniline and dicyandiamide, *Nutr. Cycling Agroecosyst.*, 1999, **54**(3), 251–257.
12 W. Zerulla, G. Pasda, R. Hähnde and A. H. Wissemeier, *The new nitrification inhibitor DMPP (ENTEC®) for use in agricultural and horticultural crops-an overview, Plant Nutrition*, Springer Netherlands, 2002, pp. 754–55.
13 G. Barth, S. V. Tucher and U. Schmidhalter, Influence of soil parameters on the effect of 3,4-dimethylpyrazole-phosphate

as a nitrification inhibitor, *Biol. Fertil. Soils*, 2001, **34**(2), 98–102.
14 Y. F. Shi, Research on the Factors Affecting Nitrification Inhibition of Dicyandiamide (DCD) in Latosol, *J. Anhui Agric. Sci.*, 2011, **12**, 1505–1508.
15 Y. Xue, Z. J. Wu and L. L. Zhang, Inhibitory effect of DMPP on soil nitrification as affected by soil moisture content, pH and organic matter, *J. Appl. Ecol.*, 2012, **23**(10), 2663–2669.
16 Y. Z. Huang, Z. W. Feng and F. Z. Zhang, Application of nitrapyrin in agriculture and environmental protection, *J. Soil Sci. Environ.*, 2001, **10**(4), 323–326.
17 L. L. Hendrickson and D. R. Keeney, Effect of some physical and chemical factors on the rate of hydrolysis of nitrapyrin (n-serve), *Soil Biol. Biochem.*, 1979, **11**(1), 47–50.
18 Z. Y. Chen, X. L. Wang and C. Y. Mi, Degradation of 2-chloro-6(trichloromethyl-^{14}C) pyridine in rice and soil, *J. Nucl. Agric.*, 1980, **24**(3), 34–39.
19 K. L. Sahrawat, D. R. Keeney and S. S. Adams, Ability of nitrapyrin, dicyandiamide and acetylene to retard nitrification in a mineral and an organic soil, *Plant Soil*, 1987, **101**(2), 179–182.
20 Y. Gu, L. H. Wu, Y. L. Liu, X. Zhang and Z. J. Wang, A preliminary study on the inhibitory effect of nitrapyrin formulations on soil nitrification, *Journal of Agro-Environment Science*, 2013, **32**(2), 251–258.
21 Z. Q. Zhang, Q. Gao, J. M. Yang, L. J. Li, Y. Li, J. H. Liu, Y. J. Wang, H. G. Su, Y. Wang, S. J. Wang and G. Z. Feng, Effect of soil organic matter on adsorption of nitrification inhibitor nitrapyrin in black soil, *Commun. Soil Sci. Plant Anal.*, 2020, (6), 1–13.
22 Z. Q. Zhang, Q. Gao, J. M. Yang, Y. Li, J. H. Liu, Y. J. Wang, H. G. Su, Y. Wang, S. J. Wang and G. Z. Feng, The adsorption and mechanism of the nitrification inhibitor nitrapyrin in different types of soils, *R. Soc. Open Sci.*, 2020, **7**, 200259.
23 E. Lipczynska-Kochany, Humic substances, their microbial interactions and effects on biological transformations of organic pollutants in water and soil: a review, *Chemosphere*, 2018, **202**, 420–437.
24 F. J. Stevenson, *Humus chemistry: genesis, composition, reactions*, 2nd edn, Wiley & Sons Ltd, New York, 1994.
25 M. H. B. Hayes, R. Mylotte and R. S. Swift, Humin: its composition and importance in soil organic matter, *Adv. Agron.*, 2017, **143**, 47–138.
26 K. S. Rawat, A. Srivastava, S. C. Bhatt, S. P. Pachauri and P. C. Srivastava, Kinetics and adsorption-desorption behavior of am nitrification inhibitor in mollisols, *Commun. Soil Sci. Plant Anal.*, 2017, **48**(8), 857–864.
27 P. A. Jacinthe and J. R. Pichtel, Interaction of nitrapyrin and dicyandiamide with soil humic compounds, *Soil Sci. Soc. Am. J.*, 1992, **56**(2), 465.
28 M. Y. Li, Y. Wang, F. Ji, K. S. Wang, A. Q. Gao, L. Wang and Z. Y. Cao, Types of Arable Soils in Jilin Province, *Journal of Northeast Agricultural Sciences*, 2016, **41**(4), 53–57.
29 X. Chen, Y. Wang, L. Zhang, X. Z. Han and J. Z. Zhang, Effects of integrated fertilizer application on nitrogen use efficiency of spring maize and soil nitrogen content on black soil in harbin, *Acta Agric. Scand., Sect. B*, 2014, **63**, 139–145.
30 Q. X. Wen, *Research Methods of Soil Organic Material (In Chinese)*, Agriculture Press, Beijing, 1984, pp. 68–106.
31 G. X. Xing, H. H. Zhang and Y. Han, Study on the nature of Fe^{3+} and Fe^{2+} bound with humic acid by Mossbauer spectroscopic method (In Chinese), *Acta Pedol. Sin.*, 1987, **24**, 218–225.
32 K. C. Li, H. B. Zhang and J. Liu, Simultaneous Determination of Pyridine, 2-Aminopyridine, 2-Methylpyridine and 2-Pyridinecarboxylic acid by Reversed Phase High Performance Liquid Chromatography, *Chin. J. Anal. Chem.*, 2005, (11), 1580–1582.
33 Z. H. Chen and X. S. Hu, A study on the preparation of 2-chloro-6-(trichloromethyl) pyridine, *Fine Chem. Intermed.*, 2009, **39**(03), 21–24.
34 H. G. Su, Z. Z. Zhang, J. H. Liu, Q. Li, J. H. Li, M. M. Zhou and J. M. Yang, Determination of Nitrapyrin in Soil by Ultrasonic Extraction and High Performance Liquid Chromatography, *Journal of Jilin University*, 2020, **58**(3), 718–724.
35 Z. Maznah, M. Halimah, I. B. Sahid and A. S. Idris, Adsorption-Desorption of Hexaconazole in Soils with Respect to Soil Properties, Temperature, and pH, *Journal of Agriculture-Food Science and Technology*, 2016, **4**(6), 493–497.
36 K. S. Rawat, A. Srivastava, S. C. Bhatt, S. P. Pachauri and P. C. Srivastava, Kinetics and Adsorption-Desorption Behavior of AM Nitrification Inhibitor in Mollisols, *Commun. Soil Sci. Plant Anal.*, 2017, **48**(8), 857–864.
37 G. Palma, R. Demanet, M. Jorquera, M. L. Mora, G. Briceño and A. Violante, Effect of pH on sorption kinetic process of acidic herbicides in a volcanic soil, *J. Soil Sci. Plant Nutr.*, 2015, **15**(3), 549–560.
38 A. Baglieri, N. Michele, F. Trotta, P. Bracco and M. Gennari, Organo-clays and nanosponges for acquifer bioremediation: adsorption and degradation of triclopyr, *J. Environ. Sci. Health, Part B*, 2013, **48**(9), 784–792.
39 X. Liu, S. Lu, Y. Liu, W. Meng and B. H. Zheng, Adsorption of sulfamethoxazole (SMZ) and ciprofloxacin (CIP) by humic acid (HA): characteristics and mechanism, *RSC Adv.*, 2017, **7**(80), 50449–50458.
40 C. Q. Huang, X. Zhang, D. C. Qiu and H. J. Chuan, Research on adsorption of methylene blue onto the mesoporous silica microspheres, *Adv. Mater. Res.*, 2012, **557–559**(1), 427–433.
41 X. M. Xiao, F. Tian, Y. J. Yan, Z. L. Wu, Z. S. Wu and G. Cravotto, Adsorption behavior of phenanthrene onto coal-based activated carbon prepared by microwave activation, *Korean J. Chem. Eng.*, 2015, **32**(6), 1129–1136.
42 L. Vincenzo, I. Pasquale, S. Stefano and C. Sante, Sorption of non-ionic organic pollutants onto a humic acids-zeolitic tuff adduct: thermodynamic aspects, *Chemosphere*, 2014, **95**, 75–80.
43 X. T. Guo, J. H. Ge, C. Yang and R. R. Wu, Sorption behavior of tylosin and sulfamethazine on humic acid: kinetic and thermodynamic studies, *RSC Adv.*, 2015, **5**(72), 58865–58872.
44 E. Çalışkan and S. Göktürk, Adsorption characteristics of sulfamethoxazole and metronidazole on activated carbon, *Sep. Sci. Technol.*, 2010, **45**(2), 244–255.

45 S. Dong, S. Dou, M. Shao, Y. Jin, L. Li, C. Tan and C. Lin, Effect of Corn Stover Deep Incorporation with Different Years on Composition of Soil Humus and Structural Characteristics of Humic Acid in Black Soil, *Acta Pedol. Sin.*, 2017, **54**(01), 150–159.

46 G. Zhang, S. Dou, Z. B. Xie, S. L. Zhong, X. Y. Yang, X. Zhou, X. Liu, X. L. Tian, F. R. Meng and X. B. Yin, Effect of biochar application on composition of soil humus and structural characteristics of humic acid, *Acta Sci. Circumstantiae*, 2016, **36**(2), 614–620.